HHS Public Access

Author manuscript

Prostate. Author manuscript; available in PMC 2019 November 04.

Published in final edited form as:

Prostate. 2016 June ; 76(8): 722–734. doi:10.1002/pros.23161.

Coordinated Induction of Cell Survival Signaling in the Inflamed Microenvironment of the Prostate

David W. McIlwain[1], **Marloes Zoetemelk**[2], **Jason D. Myers**[1], **Marshé T. Edwards**[3], **Brandy M. Snider**[1], **Travis J. Jerde**[1,4,*]

[1]Department of Pharmacology and Toxicology, Indiana University School of Medicine, Indianapolis, Indiana [2]Inholland University, Hoofddorp, Netherlands [3]Bennett College, Greensboro, North Carolina [4]Melvin and Bren Simon Cancer Center-Indiana Basic Urological Research Working Group, Indiana University, Indianapolis, Indiana

Abstract

PURPOSE—Both prostate cancer and benign prostatic hyperplasia are associated with inflammatory microenvironments. Inflammation is damaging to tissues, but it is unclear how the inflammatory microenvironment protects specialized epithelial cells that function to proliferate and repair the tissue. The objective of this study is to characterize the cell death and cell survival response of the prostatic epithelium in response to inflammation.

METHODS—We assessed induction of cell death (TNF, TRAIL, TWEAK, FasL) and cell survival factors (IGFs, hedgehogs, IL–6, FGFs, and TGFs) in inflamed and control mouse prostates by ELISA. Cell death mechanisms were determined by immunoblotting and immunofluorescence for cleavage of caspases and TUNEL. Survival pathway activation was assessed by immunoblotting and immunofluorescence for Mcl–1, Bcl–2, Bcl–XL, and survivin. Autophagy was determined by immunoblotting and immunofluorescence for free and membrane associated light chain 3 (LC–3).

RESULTS—Cleavage of all four caspases was significantly increased during the first 2 days of inflammation, and survival protein expression was substantially increased subsequently, maximizing at 3 days. By 5 days of inflammation, 50% of prostatic epithelial cells expressed survivin. Autophagy was also evident during the recovery phase (3 days). Finally, immunofluorescent staining of *human* specimens indicates strong activation of survival proteins juxtaposed to inflammation in inflamed prostate specimens.

CONCLUSIONS—The prostate responds to deleterious inflammation with induction of cell survival mechanisms, most notably survivin and autophagy, demonstrating a coordinated induction

*Correspondence to: Travis J. Jerde, Ph.D., Assistant Professor of Pharmacology and Toxicology, A417 VanNuys Medical Sciences Building, 635 Barnhill Drive, Indianapolis, IN 46202. tjjerde@iupui.edu.

Conflicts of interest: none.

AUTHORS' CONTRIBUTIONS

McIlwain, Zoetemelk, Myers, and Jerde participated in research design. Experiments was conducted by McIlwain, Zoetemelk, Myers, Edwards, Snider, and Jerde. McIlwain, Zoetemelk, Edwards, Snider, Myers, and Jerde performed data analysis. McIlwain, Snider, and Jerde wrote and contributed to the writing of the manuscript.

of survival factors that protects and expands a specialized set of prostatic epithelial cells as part of the repair and recovery process during inflammation.

Keywords

prostate; inflammation; cell survival; cell death; repair

INTRODUCTION

Continual and recalcitrant inflammation is an extremely common condition in the human prostate and has been found to be associated with a number of prostatic diseases including prostate cancer and benign prostatic hyperplasia (BPH) [1–4]. Prostatic inflammation is characterized by the presence of inflammatory cells in the stroma, epithelium, and lumen of prostatic glands where the infiltrate is primarily lymphocytic with secondary accompanying macrophages juxtaposed to loci of reactive hyperplasia [1]. The origins of inflammation in the prostate remain a subject of debate and are most likely multi-factorial [5]. A role for a bacterial component in prostatic inflammation is controversial but is certainly plausible [6–9], and colonization by non-culturable organisms has been suggested by PCR assays of bacterial 16S ribosomal RNA in prostate biopsies as this has been associated with histological evidence of inflammation [10]. Numerous nonbacterial causes of inflammation have been investigated including viruses, environmental components, systemic hormones, and urinary reflux. Whatever the cause, inflammation in the prostate is of considerable importance to urological research due to the prevalence and impacts of BPH and prostate cancer.

While much has been described regarding prostate disease resulting from oxygen and nitrogen radicals during inflammation, proliferative mechanisms associated with repair and regeneration are less understood. Repair and regrowth are co-regulated processes characteristic of many cellular responses to trauma and in order for tissue recovery to proceed, inflammation must orchestrate precise series of events directing damaged cells to die, inducing proliferation of protected tissue progenitors to repopulate damaged tissue, and promoting differentiation of those expanded cells into proper cell subtypes [11]. Errors in these processes allow for expansion of damaged cells in an environment saturated in growth promoting factors leading to hyperplasia and desmoplasia [12]. While there is an extensive literature in prostate cancer cells regarding survival and cell death escape, mechanisms of how inflammation directs cells to avoid death and proliferate are poorly understood.

In addition to the classically understood mechanisms by which cells survive noxious tissue conditions—inhibition of pro-apoptotic proteins, induction of pro-survival proteins, and the subsequent inactivation of caspases—autophagy represents a process that can be associated with both the promotion of apoptosis and the promotion of cell survival and proliferation. Autophagy consists of autophagosome formation and effective macromolecule degradation [13]. The mechanisms of autophagy are diverse and depend on the origin of the stimulus. Autophagy is implicated in a number of diseases including cancer [14]. The removal of damaged organelles or proteins can be advantageous for a cell and may act as an escape mechanism from cell death [15].

It is not known how specialized cells in the prostatic epithelium are programmed to avoid cell death mechanisms in the noxious condition of inflammation and survive in order to repopulate the tissue as part of the innate repair and recovery process. In this study, we characterize the immediate induction of cell death mechanisms in our mouse model of prostatic inflammation that has been shown to transition from acute to chronic phases of inflammation similar to human prostates. Cell death signaling induction is followed by a coordinated induction of survival mechanisms that begin in basal epithelial cells and expand to include all layers of the epithelium. We also found that autophagy is induced during the recovery phases of inflammation. Finally, we found that the most consistently induced of the survival proteins, survivin, is associated with inflammation in human prostate specimens, and that survivin expression is more tightly correlated with inflammation than with disease state of the prostate.

METHODS

In Vivo Induction of Inflammation

All animal experiments were conducted under the approval and supervision of the Indiana University School of Medicine Animal Care and Use Committee, and in accordance of National Institutes of Health guidelines for animal research. *Escherichia coli* strain 1677 (2×10^6/ml, 100 μl per mouse) was instilled through catheters into the urinary tract of C57BL/6J wild-type mice, as previously described [5,6,16]. Mice were then inoculated with 100 μl of BrdU (3.1 mg/ml Roche) for 2 hr before being sacrificed daily for 7 days after instillation, and their prostates were removed and separated by lobe (Ventral Prostate [VP], Coagulating Gland [CG], and Dorsolateral Prostate [DLP]) for molecular or histological analysis. PBS (Phosphate-buffered saline)-instilled animals were used as controls. Tissues were either paraffin-embedded for immunohistochemistical analysis or snap-frozen for molecular analysis. The *E. coli* strain 1667 in these experiments is being utilized as a tool for the induction of inflammation in the rodent prostate and has been shown to induce cellular effects that parallel that of inflammation found in a number of human prostatic diseases. In this model, the inflammatory response to bacterial inoculation is characterized by a primarily neutrophilic infiltrate in the first and second day that progresses to a primarily lymphocytic infiltrate 3–5 days post-inoculation. Macrophages are prevalent to a lesser degree throughout both acute and chronic stages. The chronic stage (days 3–5) has a very similar leukocytic content and distribution as that found in chronic human prostatic inflammation in benign or cancerous prostates [17,18]. The dorsolateral lobe of the rodent prostate has been demonstrated to produce the most dynamic and consistent response to induction of inflammation [6], and upon verification of this via tissue damage assessment, we therefore used this lobe for the molecular analysis of this study. For all experiments this model is used for (protein, histology, IF, etc.), dorsal-lateral prostates from six separate mice are used as separate data points.

Protein Localization Via Immunohistochemistry

Prostate lobes were fixed in 10% formalin overnight, processed routinely, embedded in paraffin, and serially sectioned at 5 μm with a microtome. Tissues were subjected to heat-induced antigen retrieval in 10 mM citrate buffer (citrate buffer stock solution of

monohydrate-free acid citric acid, sodium citrate dehydrate, pH 6.0) for 10 min. Sections were blocked at room temperature with a bovine serum albumin (BSA)-serum mixture for 2 hr and incubated with primary antibody overnight at 4°C. Primary antibodies and dilutions included BrdU labeling Detection kit II (1:20, Roche), rabbit anti-Cleaved Caspase 3 (1:400, Cell Signaling Technologies, Danvers, MA), rabbit anti-Cleaved Caspase 7 (1:400, Cell Signaling Technologies), rabbit anti-Cleaved Caspase 9 (1:400, Cell Signaling Technologies), rabbit anti-survivin (1:100, Cell Signaling Technologies), rabbit anti-LC3 (1:200, Cell Signaling Technologies), and mouse CD45 (1:100, Cell Signaling Technologies). Sections were washed with PBS (Phosphate-buffered saline)-Tween and incubated with IgG Alexa 488 and IgG Alexa 594-conjugated secondary antibody against rabbit or mouse for 1 hr at room temperature (1:100, Invitrogen), followed by 10 min incubation with Hoechst 33258 nuclear stain (1 μg/ml). Tissues were washed and covered with an aqueous medium and glass coverslips. The sections were analyzed by immunofluorescence and the number of positive- and negative-stained cells was determined.

Protein Quantification Via Immunoblotting

Prostate tissues were homogenized in lysis buffer containing protease inhibitor (150 mM NaCl, 10 mM tris, 1 mM EDTA, 1 mM benzenesulfonyl fluoride, and 10 μg/ml each of aprotinin, bestatin, L-luecine, and pepstatin A) and 1% Triton X-100. The homogenate was centrifuged for 20 min at 14,100*g* at 4 °C and the supernatant was collected and total protein concentration was determined by BCA (bicinchoninic acid) assay (Pierce, Rockford, IL). A total of 20 μg/well of Protein were resolved by electrophoresis in 4–15% gradient polyacrylamide gels. Proteins were transferred to polyvinylidene difluoride membranes, blocked for 24 hr [(10% Dry milk, 5% BSA, 0.05% NaN_3) in 1xPBS(2.7 mM KCl, 1.5 mM KH_2PO_4, 136 mM NaCl, 8 mM Na_2HPO_4)-Tween 20] and incubated overnight with one of the following primary antibodies: mouse β-actin (1:1000, Cell Signaling Technologies), rabbit survivin (1:1000, Cell Signaling Technologies), rabbit Bcl-2 (1:1000, Cell Signaling Technologies), rabbit Mcl-1 (1:500, Cell Signaling Technologies), and rabbit LC3 (1:1000, Cell Signaling Technologies). After blots were washed six times with PBS-Tween, blots were incubated with donkey antibody against rabbit immunoglobulin G conjugated to horseradish peroxidase for 1 hr (1:200,000 dilution, Pierce) in nonfat dry milk, PBS, and 0.05% Tween 20. Peroxidase activity was detected via West Femto chemiluminescence reagent (Pierce). Photo images were analyzed by densitometry.

Cell Death/Survival Factors Expression Via ELISA

Prostate tissues were harvested and homogenized from 8-week-old C57BL/6J WT mice 0–14 days after uropathogenic *E. coli* strain 1677 instillation. For release experiments, tissues were equilibrated for 1 hr in aerated Krebs physiological salt solution, with buffer changes of 15 min and then 30 min. Krebs was collected after the experiment and frozen as the "released fraction." Additional tissues were harvested for the total tissue content, and these tissues were snap frozen in liquid nitrogen, placed in sterile PBS, and homogenized. Tissue slurries were centrifuged at 14,000*g* for 10 min and the supernatant was collected as the total tissue content fraction. All collections were analyzed by ELISA for TNF, TWEAK, TRAIL, FAS-Ligand, Shh, IGF-α, IL-1β, IL-6, TGF-β1, and TGF-β3 as recommended by the manufacturer (Biosource; Camarillo, CA). Absorbance readings for each concentration were

normalized as a ratio to control non-inflamed prostates. Comparisons between inflammatory time points are expressed as mean ±s.e.m. $^{*}P<0.05$ versus PBS-instilled prostate; using analysis of variance (ANOVA).

DNA Fragmentation Via TUNEL

Prostate lobes were fixed in 10% formalin overnight, processed and embedded in paraffin and serially sectioned at 5 μm with a microtome and rehydrated as previously mentioned. Tissue sections were incubated with Proteinase K working solution (10 μg/ml in 10 nM Tris/HCl, pH 7.4–8) at RT for 15 min and then rinsed twice with PBS. Fifty micro-litre of TUNEL reaction mixture (In Situ Cell Death Detection Kit Fluorescein, Roche Applied Science) were added to each section and slides were placed in a humidified atmosphere for 60 min at 37°C in the dark. The slides were then rinsed three times with PBS and stained with Hoechst 33,258 as previously described. Tissues were then washed and covered with an aqueous medium and glass coverslips. Samples were directly analyzed under a fluorescence microscope using an excitation wavelength in the range of 450–500 nm and detection in the range of 515–565 nm (green).

Human Specimens

Human specimens were obtained with appropriate minimal risk institutional review board approval according to the approval and guidelines at Indiana University School of Medicine. Sections were cut from pre-existing paraffin-embedded human prostate tissues obtained as part of a transurethral resection of the prostate (TURP), a prostatectomy, or from prostate specimens removed collaterally from bladder cancer patients undergoing radical cystectomy (cystoprostatectomy) as control human specimens. These controls were age-matched to the BPH-TURP and prostate cancer specimens, and were verified by record to be naïve for infection or pretreatment with Bacillus Calmette-Guérin as first-line therapy because these patients had presented with muscle invasive bladder cancer. Further, the controls were not exhibiting benign prostatic hyperplasia symptoms and were verified by pathology to be prostate cancer free. Control regions from both the transition zone and peripheral zone were used for analysis as controls for both BPH and prostate cancer, respectively. There were prostates collected from 12 separate patients used for this study. For calculation, five random 20× views were analyzed for survivin and CD45 positive cells and averaged for each separate data point.

The age range of specimens is 45–72, with the average age of 64 for BPH specimens, 66 for control prostates, and 68 for prostate cancer specimens. Prostate cancer specimens were all Gleason 3+3, 3 +4, or 4 +3. All human specimens were stained with survivin and CD45 antibodies for immunofluorescence, as described above.

RESULTS

Inflammation Causes Tissue Damage and Hyperplasia in a Model of Prostatic Inflammation

Mice instilled with uropathogenic *E. coli* 1677 exhibited widespread inflammation with varying degrees of hyperplasia and dysplasia consistent with previous papers on this model, and as has been previously published, the dorsolateral lobe of the prostate produced the most

consistent and dynamic response to inflammation [6,16]. Three days after instillation, WT animal epithelium develops distinct multilayers and display extensive inflammatory infiltrate (Fig. 1). Previous reports from this model indicate that the inflammatory infiltrate in this model is primarily neutrophilic 1–2 days post induction, and lymphocytic 3–5 days after inflammation with accompanying macrophages [6,16]. This phase mimics what is observed in human prostates with chronic inflammation [17,18]. Intense loci of inflammation are juxtaposed to epithelial hyperplasia and the prostatic glands juxtaposed to intense inflammation show tremendously increased epithelial cell proliferation and hyperplasia. Mice exhibiting 1–3 days of inflammation exhibit numerous damaged and apoptotic cells as evidenced by pyknotic nuclei and retracted cytoplasm (Fig. 1). These data demonstrate that our model of prostatic inflammation is associated with the damaging effects of inflammation and cellular damage.

Inflammation Causes Rapid Apoptotic Response

To characterize inflammation-induced apoptosis, we assessed control and inflamed mouse prostates for expression of executioner caspase 3, 7, and 6 cleavage via immunohistochemistry (Fig. 2A and B). We found an increase in cells exhibiting activation (cleavage) of all three executioner caspases with caspase 3 being the most dramatic, peaking at day 2 with 1.3% of cells expressing cleaved caspase 3 (n =6 mice). Cleaved caspase 3 positive cells were primarily found in select basal and luminal epithelial cells of prostatic glands and absent from the fibromuscular stroma. In addition, we assessed these tissues for later stage apoptosis by staining for nick-end labeling of fragmented DNA. To determine this, a terminal deoxynucleotidyl transferase dUTP nick-end labeling (TUNEL) was performed to measure percent of epithelial cells in later stage apoptosis as described in histologic sections of prostate tissue and positive cells were detected by fluorescent microscopy (Fig. 2C). Few fluorescein-positive cells were found in days 0 and 1 of infection but a significant increase in apoptotic cells was found in day 2 with subsequent decrease by day 4. The fluorescein positive cells, like the caspase 3 positive cells, were primarily found in the basal and luminal compartments of the prostatic glands.

Inflammation Induces Death and Survival Factor Production and Release

Inflammation induces coordinated and temporal expression and release of known cell death factors, subsequently followed by an induction of a panel of known cell survival-inducing factors. As measured by ELISA, bona fide cell death-inducing mediators TNFα, TWEAK, TRAIL, and FAS ligand are all induced rapidly and transiently upon induction of acute inflammation in the dorsolateral prostate, maximizing at 1–2 days after induction (Fig. 3A and B). Subsequent to induction of death ligands, the production of known cell survival factors Shh, IGF-1, IL-1α, IL-6, TGFβ1, and TGFβ2 are substantially induced in the second day of inflammation, and maximizes at day 3 (Fig. 3C and D, n =6 mice). IL-1α, IL-6, and TGFβ1 remained significantly induced for 5 days after inflammation induction. These data demonstrate that death factors coincide with the acute and neutrophilic phase of inflammation, and are coordinately followed by the induction of survival factors corresponding to the lymphocytic phase of inflammation.

Inflammation Induces Cell Survival Signaling Pathways in Response to Apoptotic Signals

We assessed the induction of four previously identified survival signaling molecules, previously known to regulate cell survival in prostate cells: survivin, Bcl-2, Bcl-XL, and Mcl-1 (Fig. 4). Our data indicate that inflammation induces the expression of survivin, Bcl-2 and Mcl-1, but had no effect on Bcl-XL expression (Not shown). The most prominently induced survival protein by inflammation was survivin, exhibiting an eightfold induction at days 3 and 4 after inflammation relative to uninflamed control prostates (Fig. 4A and B; n =6 mice). Since survivin was the most dynamic and consistently induced survival factor in inflamed prostates, we sought to further characterize its induction. Survivin is rarely expressed in control prostates, being expressed in 1% of epithelial cells, and primarily in select basal cells (Fig. 4C-top). Immunofluorescence of survivin expression increased linearly by day throughout the first 5 days of inflammation (Fig. 4D), and by 5 days 50% of the epithelial cells of inflamed prostates were positive for survivin (Fig. 4D), image depicted in Figure 4C-bottom. The percentage of survivin-positive cells remained increased for 7 days of infection. These data indicate that survival proteins are induced during prostatic inflammation, corresponding to induced survival factor signals and the lymphocytic phase of inflammation, and temporally following the neutrophilic death factor/apoptotic phase.

Inflammation Induces Autophagy: LC 3 Association With the Autophagosome

As autophagy is a cell mechanism that can lead to either cell survival or cell death, we sought to characterize its induction in prostatic inflammation. Inflammation increases both the expression and vesicle association of the autophagy LC3 (Fig. 5). LC3 is expressed in the cytosol of cells and, upon initiation of autophagy, LC3 associates with vesicular membranes to form the autophagosome. This causes LC3 to run faster on gels, so a lower running band in immunoblotting is indicative of autophagosome-associated LC3, and therefore autophagy induction. Immunoblotting of proteins from inflamed prostates demonstrates that autophagy is induced by inflammation in the prostate, maximizing at 3 days of inflammation (Fig. 5A and B; n =6 mice). Additionally, LC3 expression itself is also induced after three days of inflammation. To further characterize LC3 during prostatic inflammation, we assessed tissue localization by in immunofluorescence. Autophagosome-associated LC3 is associated with a punctate appearance as the protein is concentrated around the vesicle (Fig. 5C). We found that the number of prostatic epithelial cells exhibiting punctate LC3 increased from 4% of epithelial cells to 25% by the third day of inflammation (Fig. 5D). Autophagic cells were found throughout the epithelium, in both luminal and basal layers. These data demonstrate that the potentially cell survival mechanism of autophagy is induced by acute prostatic inflammation, and maximizes during the lymphocytic phase.

Survivin Is Induced Juxtaposed to Inflammation in Human Prostate Specimens

In our in vivo mouse model of prostatic inflammation, survivin is the most consistently induced survival factor in the prostate in response to inflammatory signals. Because of this, we sought to determine if it is induced by inflammation in human prostate specimens. To address inflammation and survival protein expression in human tissue, we co-stained for $CD45^{+}$ (immune cells) and survivin in non-diseased (prostates removed from cystectomies),

BPH specimens (via TURP), and prostate cancer specimens (removed via prostatectomy), 12 tissues (from 12 separate patients) per group. As previously reported, survivin is induced in the majority of prostate cancer specimens, and is not expressed in the majority of non-diseased control prostates. However, our staining also demonstrated that regions of inflammation associated with survivin induction regardless of whether the region was found in non-diseased or diseased prostates (Fig. 6). We defined both inflamed and non-inflamed regions in all three prostatic conditions (non-diseased, BPH, and cancer) by the number of CD45-evident 20× fields. Based on our previously established mouse model inflammatory scoring [6], we set the criteria for inflammation to be greater than or equal to 30 $CD45^+$ cells per 20× field, and non-inflamed regions were defined as less than 10 $CD45^+$ cells per field. Using this criteria, we quantified the number of survivin-positive cells in sections from inflamed and non-inflamed regions in non-diseased, BPH, and cancerous prostate specimens. We found that regardless of condition, inflamed fields were associated with 60–70% of epithelial cells positive for survivin, while non-inflamed non-diseased and BPH fields exhibited less than 10% of epithelial cells positive for survivin, and non-inflamed cancerous fields were associated with 24% positive cells (Fig. 6B). While there was a threefold increase in survivin-positivity among prostate cancer specimens independent of inflammation, the primary difference between diseased and non-diseased prostates was the prevalence of inflammation (Fig. 6C). In non-diseased prostates, severe inflammation represented on average 11% of sections, while in BPH and prostate cancer sections severe inflammation constituted 82% and 71% of the section, respectively. There was no difference in the severity of inflammation in the 20× views quantified in this study once they were determined to be in the “severe” (>30 CD45-positive leukocytes per field) category. Additionally, we observed no significant difference in survivin-positivity between the transition zone and peripheral zone of non-diseased prostates.

DISCUSSION

Inflammation is a common feature of prostate biology and is believed to be associated with the disease progression involved in both BPH and prostate cancer. Yet, inflammation is also a destructive process that involves a repair and recovery stage in which protected cells must survive the initial insults of inflammation, followed by their rapid proliferation as a means to repopulate the damaged tissue. The cell signaling mechanisms involved in coordinating these events is not understood, and little is known as to how the epithelium of tubular structures such as the prostate protects the specialized cells that are the keystones of epithelial repair and recovery.

The data in the present study indicate that inflammation induces a profile of cell death and cell survival-inducing factors, coordinated such that death factors and induction of cell death cellular mechanisms occurs within the first 48 hr after induction of inflammation, followed by a maximized expression of survival factors and signaling pathways. Inflammation causes visible death of the prostatic epithelium in the first 48 hr of inflammation as evidenced by H&E staining and confirmed by activation of caspases and nick-end labeling. Coordinate with this, there is a significant induction of cell death factors including TNFα, TWEAK, TRAIL, and FasL. Secondary to cell death, the acute inflammation time course exhibits induction of known survival factors including growth factors, cytokines, and developmental

morphogens that correspond to activation of survival pathways that include survivin, Mcl-1, and Bcl-2. We conclude from this that a population of epithelial cells resides in the prostatic epithelium that responds to inflammatory signals by inducing survival factors, and functions to repopulate the tissue during repair secondary to the damaging effects of inflammatory triggers.

Additionally, autophagy mechanisms maximize during this survival phase and may represent an additional cell survival mechanism in prostatic epithelial cells. Autophagy is indicated by the formation of autophagosomes for cell protein digestion during stress. Cells in autophagy can either use the digested material for survival, or they can be entered into the apoptotic cascade if the stress time period endures. During the induction of autophagy, the normally cytosolic protein Light Chain 3 (LC3) associates and participates in the formation of the autophagosome. As such, the association of LC3 in a lipid fraction—that of a membrane—indicates the induction of autophagy. In our study, autophagosome-associated LC3 was evident by two methods: the faster-running band at 14 KD in immunoblotting that indicates autophagosome association; secondly, the specific exhibition of LC3 into punctate formations indicating the presence of autophagosomes. Our data demonstrate a substantial increase in the faster running band by immunoblotting, and in the number of epithelial cells exhibiting punctate LC3 containing autophagosomes. From this we conclude that inflammation induces autophagy in a subset of prostate epithelial cells in experimental models of prostatic inflammation.

The mouse model used in this study is a model of acute inflammation that progresses to chronic inflammation. This is characterized by an early neutrophilic infiltrate that dominates in the first 2 days of induction, and progresses to a primarily lymphocytic and monocytic infiltrate in days 3–5. This later lymphocytic chronic stage of the inflammatory response has a cellular infiltrate and an expression profile consistent to what is observed in human chronically inflamed prostates. The time course of cellular infiltrate in this model exhibits remarkably little experimental variation error, demonstrating that the time course of the inflammatory response is highly reproducible and consistent. Further, inflammation in this model was accompanied by increased expression of several inflammatory mediators and gene products including IL-1 family members, IL-6, COX-2, IGF-1, and FGFs, commonly observed in chronic prostatic inflammation. Therefore it is not unexpected that an increase in survival protein expression occurs during the chronic phase of this model, just as is observed in human chronically inflamed prostates.

Survivin was the most consistent and substantially induced of the survival proteins in our mouse study, and we sought to validate its responsiveness to inflammation in human specimens. While the expression of survivin is well-known to be induced in both BPH and prostate cancer [19–21], this is the first report we are aware of in which survivin localization is characterized juxtaposed to inflammation. We found that survivin expression does localize to areas of severe inflammation, but what was striking is how this localization is largely disease-independent. There was no difference in the number of survivin-positive cells in inflamed regions between BPH, cancer, and non-diseased regions; the primary discriminating factor between the pathological states is how widespread inflammation is in each state. Severe inflammation was present in over 80% of our BPH sections and over 70%

of our prostate cancer specimens, but was only a feature in less than 15% of non-diseased sections. Inflammation was associated with reactive hyperplasia and stromal desmoplasia in all tissues where it was present, but there was no consistent formation of any pre-malignant epithelial lesions such as dysplasia in inflamed regions of non-diseased prostates. We propose that the previously published findings describing high survivin localization in diseased prostates is in large part a factor of the increased inflammation in those specimens. It must be noted, however, that in those uncommon regions of prostate cancer that are not associated with inflammatory infiltrate, there is still an increased number of survivin-positive cells, independent of inflammation. Therefore we conclude that prostate cancer does have intrinsic survivin induction relative to benign epithelium, but this is still enhanced with inflammation. BPH specimens did not exhibit any increase, absent of inflammation.

There is a clear association of BPH with inflammation, both in proliferating cells and in association with symptoms. The prevalence of inflammation in BPH specimens is repeatedly reported to be found in between 75% and 100% of specimens. A well-characterized study by Nickel et al. reported substantial prostatic inflammation in 100% of 80 men undergoing prostatectomy for treatment of BPH [22], and histological examination of prostates from 8224 men enrolled in the REDUCE trial revealed inflammation in 78% of specimens [23]. Critically, histologically verified inflammation is the most tightly correlated histological finding to prostate symptomology in men with BPH [24]. Similarly, strong evidence links inflammation to the development, growth, and survival of cancer in the prostate [1]. Histopathology studies of human prostatectomy specimens identified lesions characterized by proliferating epithelial cells and activated inflammatory cells (proliferative inflammatory atrophy, PIA) in juxtaposition to areas of neoplasia. Sustained cell proliferation in the inflammatory environment rich in growth factors, activated stroma, and DNA-damage-promoting agents, could potentiate, and/or promote neoplasia. Additionally, proliferative inflammatory atrophy (PIA) is characterized by proliferating epithelial cells and is found in association with prostatic intra-epithelial neoplasia (PIN) and prostate cancer. These findings have prompted the hypothesis that chronic inflammation is involved in the genesis and/or progression of prostate cancer.

Several aberrant molecular mechanisms in apoptosis pathways have been identified to result in prostate disease, and androgen axis modulators—a mainstay of our therapies against prostate cancer growth—rely heavily on induction of apoptotic mechanisms for their efficacy [25–28]. Multiple modifications to cell death and survival pathways have been discovered in prostate tumors, BPH, and prostate cell lines that may participate in either tumorigenesis, proliferation, or therapy resistance. Increased expression of the survival proteins survivin, Bcl-2, Bcl-xL, Bcl-ω, and Mcl-1 are associated with prostate cancer and BPH, and interestingly inhibiting their expression sensitizes cells to cytotoxic therapies [29–31]. In addition, down-regulation or inhibition of these survival proteins results in increased chemosensitivity in prostate cell lines [31–33]. Finally, prostate cancer cells exhibit decreased death receptor expression and upregulated decoy death receptor expression, and this results in diminished apoptosis induction capacity [34,35]. Our present findings add to the understanding of the balance between pro-apoptotic and pro-survival signaling in prostate epithelial cells by demonstrating extrinsic control of both death factors and subsequent survival factor induction in a specialized cell population, by inflammation.

CONCLUSION

Our data indicate that prostatic tissue responds to the damaging effects of inflammation by an active induction of cell survival factors and signaling mechanisms, most notably survivin. Autophagy, a potential cell survival mechanism, is also substantially activated and these survivin-expanded cells may depend upon survival signaling. This study further suggests that there is a coordinated induction of survival factors that function to protect and expand a specialized set of prostatic epithelial cells. In human prostate, induction of survivin is juxtaposed to loci of severe inflammation induction in benign and cancerous prostates, and inflammation appears to be more acutely the inducer of this critical protein in the microenvironment than cancer itself is. Future studies will be aimed at determining if early stage prostate cancer set in inflammatory microenvironments survive the damaging effects of inflammation using these mechanisms.

Acknowledgments

Grant sponsor: National Institutes of Health-NIDDK; Grant number: DK092366-01A1; Grant sponsor: Department of Pharmacology and Toxicology; Grant sponsor: Indiana University School of Medicine Melvin and Bren Simon Cancer Center; Grant sponsor: Indiana Clinical and Translational Sciences Institute (CTSI).

The authors gratefully acknowledge Jill Fehren-bacher, Kai-Ming Chou and Yeh-Wen Chen for use and expertise in fluorescent microscopy. This work was funded by National Institutes of Health-NIDDK [DK092366-01A1], the Department of Pharmacology and Toxicology, the Indiana University School of Medicine Melvin and Bren Simon Cancer Center, Indianapolis, IN and Indiana Clinical and Translational Sciences Institute (CTSI) (DWM).

References

1. De Marzo AM, Platz E, Sutcliffe S, Xu J, Grönberg H, Drake CG, Nakai Y, Isaacs WB, Nelson WG. Inflammation in prostate carcinogenesis. Nat Rev Cancer. 2007; 7:256–269. [PubMed: 17384581]
2. Kramer G, Mitteregger D, Marberger M. Is benign prostatic hyperplasia (BPH) an immune inflammatory disease? Eur Urol. 2007; 51:1202–1216. [PubMed: 17182170]
3. Delongchamps NB, de la Roza G, Chandan V, Jones R, Sunheimer R, Threatte G, Jumbelic M, Haas GP. Evaluation of prostatitis in autopsied prostates—Is chronic inflammation more associated with benign prostatic hyperplasia or cancer? J Urol. 2008; 179(5):1736–1740. [PubMed: 18343414]
4. Sfanos KS, De Marzo AM. Prostate cancer and inflammation: The evidence. Histopathology. 2012; 60(1):199–215. [PubMed: 22212087]
5. Elkahwaji JE, Zhong W, Hopkins WJ, Bushman W. Chronic bacterial infection and inflammation incite reactive hyperplasia a mouse model of chronic prostatitis. Prostate. 2007; 67(1):14–21. [PubMed: 17075821]
6. Boehm BJ, Colopy SA, Jerde TJ, Loftus CJ, Bushman W. Acute bacterial inflammation of the mouse prostate. Prostate. 2012; 72(3):307–317. [PubMed: 21681776]
7. Cohen RJ, Shannon BA, McNeal JE, Shannon T, Garrett KL. Propionibacterium acnes associated with inflammation in radical prostatectomy specimens: A possible link to cancer evolution? J Urol. 2005; 173(6):1969–1974. [PubMed: 15879794]
8. Sfanos KS, Sauvageot J, Fedor HL, Dick JD, De Marzo AM, Isaacs WB. A molecular analysis of prokaryotic and viral DNA sequences in prostate tissue from patients with prostate cancer indicates the presence of multiple and diverse microorganisms. Prostate. 2008; 68(3):306–320. [PubMed: 18163428]
9. Sfanos KS, Isaacs WB. An evaluation of PCR primer sets used for detection of Propionibacterium acnes in prostate tissue samples. Prostate. 2008; 68(14):1492–1495. [PubMed: 18651578]
10. Hochreiter WW, Duncan JL, Schaeffer AJ. Evaluation of the bacterial flora of the prostate using a 16S rRNA gene based polymerase chain reaction. J Infect Dis. 1999; 180(4):1378–1381. [PubMed: 10479177]

11. Puchelle E, Zahm JM, Tournier JM, Coraux C. Aiwary epithelial repair, regeneration, and remodeling after injury in chronic obstructive pulmonary disease. Proc Am Thorac Soc. 2006; 3:726–733. [PubMed: 17065381]
12. Wang W, Bergh A, Damber JE. Chronic inflammation in benign prostate hyperplasia is associated with focal upregulation of cyclooxygenase-2, Bcl-2, and cell proliferation in the glandular epithelium. Prostate. 2004; 1:60–72.
13. Codogno P, Meijer AJ. Autophagy and signaling: Their role in cell survival and cell death. Cell Death Differ. 2005; 12:1509–1518. [PubMed: 16247498]
14. Yang ZJ, Chee CE, Huang S, Sinicrope FA. The role of autophagy in cancer: Therapeutic implications. Mol Cancer Ther. 2011; 10:1533. [PubMed: 21878654]
15. Rodriguez-Enriquez S, He L, Lemasters JJ. Role of mitochondrial permeability transition pores in mitochondrial autophagy. Int J Biochem Cell Biol. 2004; 36:2463–2472. [PubMed: 15325585]
16. Jerde TJ, Bushman W. IL-1 induces IGF-dependent epithelial proliferation in prostate development and reactive hyperplasia. Sci Signal. 2009; 2(86):49.
17. Theyer G, Kramer G, Assmann I, Sherwood E, Preinfalk W, Marberger M, Zechner O, Steiner GE. Phenotypic characterization of infiltrating leukocytes in benign prostatic hyperplasia. Lab Invest. 1992; 66(1):96–107. [PubMed: 1370561]
18. Robert G, Descazeaud A, Nicolaïew N, Terry S, Sirab N, Vacherot F, Maillé P, Allory Y, de la Taille A. Inflammation in benign prostatic hyperplasia: A 282 patients' immunohistochemical analysis. Prostate. 2009; 69(16):1774–1780. [PubMed: 19670242]
19. Rodríguez-Berriguete G, Fraile B, de Bethencourt FR, Prieto-Folgado A, Bartolome N, Nuñez C, Prati B, Martínez-Onsurbe P, Olmedilla G, Paniagua R, Royuela M. Role of IAPs in prostate cancer progression: Immunohistochemical study in normal and pathological (benign hyperplastic, prostatic intraepithelial neoplasia and cancer) human prostate. BMC Cancer. 2010; 10:18. [PubMed: 20078866]
20. Nastiuk KL, Krolewski JJ. FLIP-ping out: Death receptor signaling in the prostate. Cancer Biol Ther. 2008; 7:1171–1179. [PubMed: 18719361]
21. Shariat SF, Ashfaq R, Roehrborn CG, Slawin KM, Lotan Y. Expression of survivin and apoptotic biomarkers in benign prostatic hyperplasia. J Urol. 2005; 174(5):2046–2050. [PubMed: 16217391]
22. Nickel JC, Downey J, Young I, Boag S. Asymptomatic inflammation and/or infection in benign prostatic hyperplasia. BJU Int. 1999; 84(9):976–981. [PubMed: 10571623]
23. Nickel JC, Roehrborn CG, O'Leary MP, Bostwick DG, Somerville MC, Rittmaster RS. The relationship between prostate inflammation and lower urinary tract symptoms: Examination of baseline data from the REDUCE trial. Eur Urol. 2008; 54:1379–1384. [PubMed: 18036719]
24. Nickel JC. Inflammation and benign prostatic hyperplasia. Urol Clin North Am. 2008; 1:109–115.
25. Yamamoto H, Ngan CY, Monden M. Cancer cells survive with survivin. Cancer Sci. 2008; 9:1709–1714.
26. Kishi H, Igawa M, Kikuno N, Yoshino T, Urakami S, Shiina H. Expression of the survivin gene in prostate cancer: Correlation with clinicopathological characteristics, proliferative activity and apoptosis. J Urol. 2004; 171:1855–1860. [PubMed: 15076293]
27. De Nunzio C, Kramer G, Marberger M, Montironi R, Nelson W, Schröder F, Sciarra A, Tubaro A. The controversial relationship between benign prostatic hyperplasia and prostate cancer: The role of inflammation. Eur Urol. 2011; 1:106–117.
28. Cornforth AN, Davis JS, Khanifar E, Nastiuk KL, Krolewski JJ. FOXO3a mediates the androgen-dependent regulation of FLIP and contributes to TRAIL-induced apoptosis of LNCaP cells. Oncogene. 2008; 27:4422–4433. [PubMed: 18391984]
29. Sun A, Tang J, Hong Y, Song J, Terranova PF, Thrasher JB, Svojanovsky S, Wang HG, Li B. Androgen receptor-dependent regulation of Bcl-xL expression: Implication in prostate cancer progression. Prostate. 2008; 68:453–461. [PubMed: 18196538]
30. van Delft MF, Huang DC. How the Bcl-2 family of proteins interact to regulate apoptosis. Cell Res. 2006; 16:203–213. [PubMed: 16474435]
31. Nguyen M, Marcellus RC, Roulston A, Watson M, Serfass L, Murthy Madiraju SR, Goulet D, Viallet J, Bélec L, Billot X, Acoca S, Purisima E, Wiegmans A, Cluse L, Johnstone RW, Beauparlant P, Shore GC. Small molecule obatoclax (GX15-070) antagonizes Mcl-1 and

overcomes Mcl-1—Mediated resistance to apoptosis. Proc Natl Acad Sci USA. 2007; 104:19512–19517. [PubMed: 18040043]

32. Sternberg CN, Dumez H, Van Poppel H, Skoneczna I, Sella A, Daugaard G, Gil T, Graham J, Carpentier P, Calabro F, Collette L, Lacombe D. EORTC Genitourinary Tract Cancer Group. Docetaxel plus oblimersen sodium (Bcl-2 antisense oligonucleotide): An EORTC multicenter, randomized phase II study in patients with castration-resistant prostate cancer. Ann Oncol. 2009; 20:1264–1269. [PubMed: 19297314]
33. Mohammad RM, Goustin AS, Aboukameel A, Chen B, Banerjee S, Wang G, Nikolovska-Coleska Z, Wang S, Al-Katib A. Preclinical studies of TW-37, a new nonpeptidic small-molecule inhibitor of Bcl-2, in diffuse large cell lymphoma xenograft model reveal drug action on both Bcl-2 and Mcl-1. Clin Cancer Res. 2007; 13:2226–2235. [PubMed: 17404107]
34. Bova GS, MacGrogan D, Levy A, Pin SS, Bookstein R, Isaacs WB. Physical mapping of chromosome 8p22 markers and their homozygous deletion in a metastatic prostate cancer. Genomics. 1996; 35:46–54. [PubMed: 8661103]
35. Sanlioglu AD, Koksal IT, Ciftcioglu A, Baykara M, Luleci G, anlioglu SS. Differential expression of TRAIL and its receptors in benign and malignant prostate tissues. J Urol. 2007; 177:359–364. [PubMed: 17162091]

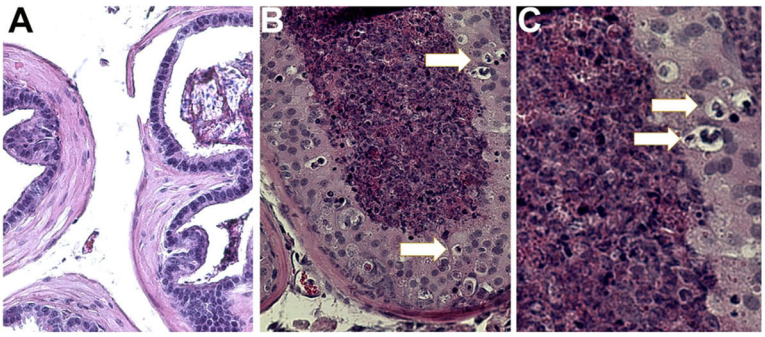

Fig. 1.

Hematoxylin and Eosin staining of 3 day inflamed dorsolateral prostates in the mouse prostatic inflammation model. **A**: (200×) Non-inflamed control prostate shows pseudostratified epithelium and very few apoptotic or autophagic cells. **B**: 200× Inflamed prostatic duct shows layering of epithelium characteristic of reactive hyperplasia during inflammation, but also shows numerous damaged and apoptotic cells as evidenced by pyknotic nuclei and retracted cytoplasm (arrows). **C**: 400× Image of damaged epithelial cells in hyperplastic epithelium in inflamed prostate.

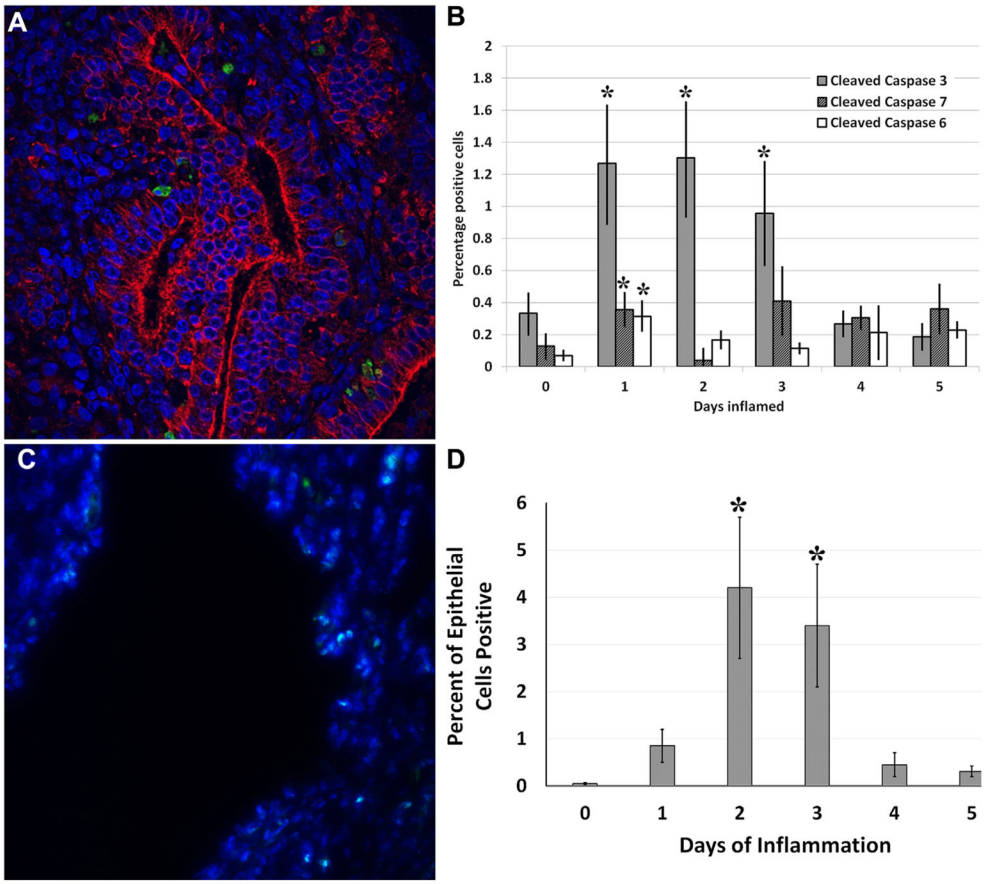

Fig. 2.

Inflammation of the mouse prostate results in induced apoptotic signaling. **A**: Fluorescent image (200×) of cleaved caspase 3 (green) in the epithelium (PanCK-red) of mouse prostates inflamed 3 days. **B**: Calculated data of epithelial cells for cleaved caspases 3, 7, and 6 from 6 mouse dorsal-lateral prostate lobes inflamed to the time points shown, expressed as percentage of cleaved caspase-positive cells within the epithelial compartment. **C**: Fluorescent image (200×) of TUNEL-positive cells. **D**: Calculated data of epithelial cells for TUNEL from 6 mouse dorsal-lateral prostate lobes inflamed to the time points shown, expressed as percentage of TUNEL-positive cells within the epithelial compartment. All data are expressed as mean ±s.e.m. $^{*}P<0.05$ versus PBS-instilled prostate; comparisons using analysis of variance (ANOVA), n =6.

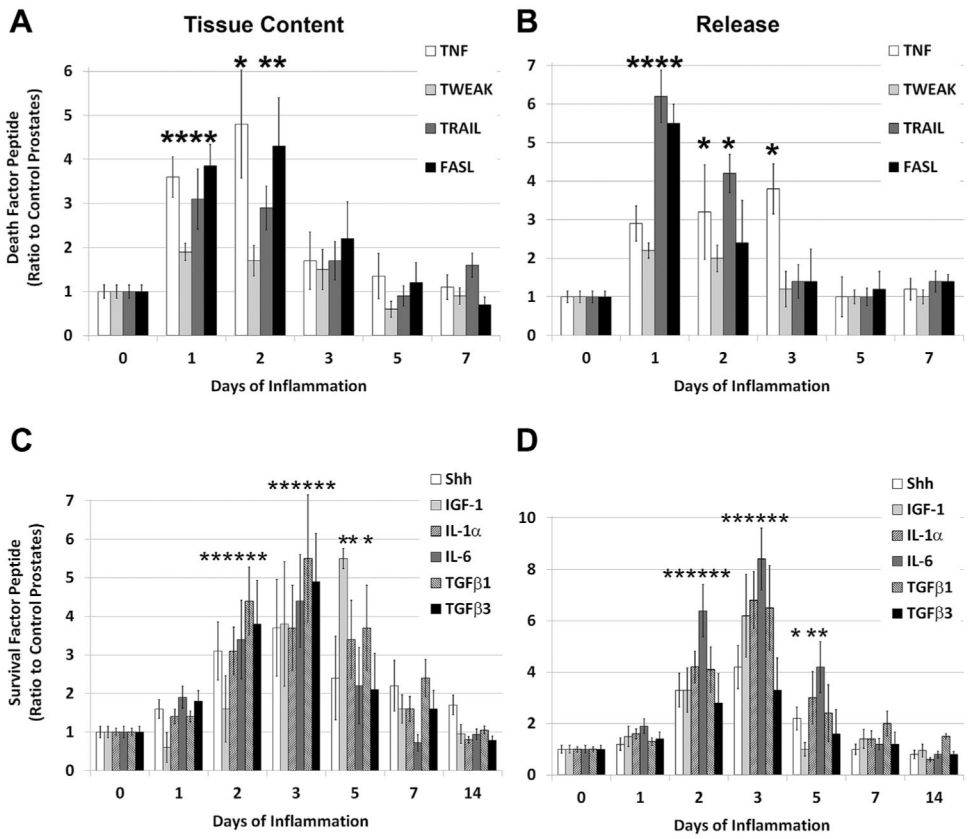

Fig. 3.

Inflammation induces the expression and release of known cell death factors, followed by an induction of a panel of known cell survival-inducing factors. **A**: Total tissue content of TNFα, TWEAK, TRAIL, and FAS ligand are all induced rapidly upon induction of inflammation in the dorsolateral prostate, maximizing at 1–2 days after induction. **B**: Correspondingly, the released fraction of these death ligands increases, indicating that release of the factor occurs allowing their function. **C**: Subsequently, the induction of known cell survival factors Shh, IGF-1, IL-1α, IL-6, TGFβ1, and TGFβ2 begins in the second day of inflammation, and maximizes at day 3. IL-1α, IL-6, and TGFβ1 remained induced for 5 days after inflammation induction. **D**: The released fraction of cell survival factors increases correspondingly to their production. All peptides were assessed by ELISA of whole dorsolateral prostate lobes and calculated as picogram of peptide per gram of tissue. Data were then normalized as a ratio to control non-inflamed prostates at the given time point of induction, for presentation. All data are expressed as mean ±s.e.m. $^{*}P<0.05$ versus PBS-instilled prostate; comparisons using analysis of variance (ANOVA), n =6. Asterisk-labeled time points are those that show significant inducibility of all death or survival factors.

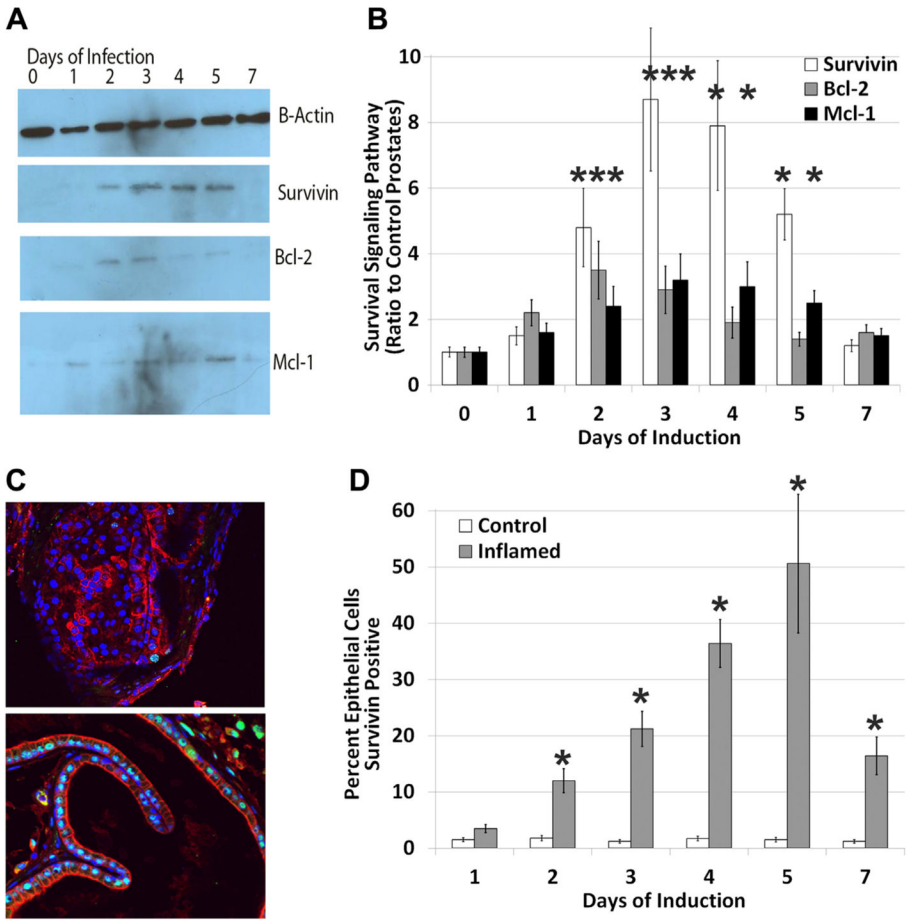

Fig. 4.

Inflammation induces three primary cell survival signaling pathways in mouse dorsolateral prostates, most prominently, survivin. **A**: Immunoblot example of induction of survivin, Bcl-2, and Mcl-1 during the time course of inflammation in mouse prostates. **B**: Quantified data of relative expression of all three survival proteins during prostatic inflammation; data were calculated as ratio of pixel intensity of the given survival protein, relative to β-actin, and expressed as ratio of expression to control prostates at the corresponding time of induction. Data are expressed as mean ±s.e.m. $^{*}P<0.05$ versus PBS-instilled (control) prostate; comparisons using analysis of variance (ANOVA), n =6. **C**: Immunofluorescence of survivin expression (green) in 5 day instilled control (top) and inflamed (bottom) dorsolateral prostates demonstrating epithelial cell (PanCK, red) expression in the nucleus during inflammation. **D**: Quantified cell counting of epithelial cells positive for survivin expression; data expressed are the percentage of epithelial cells expressing survivin in control and inflamed prostates at each time point of inflammation. All data are expressed as mean ±s.e.m. $^{*}P<0.05$ versus PBS-instilled prostate; comparisons using analysis of variance (ANOVA), n =6.

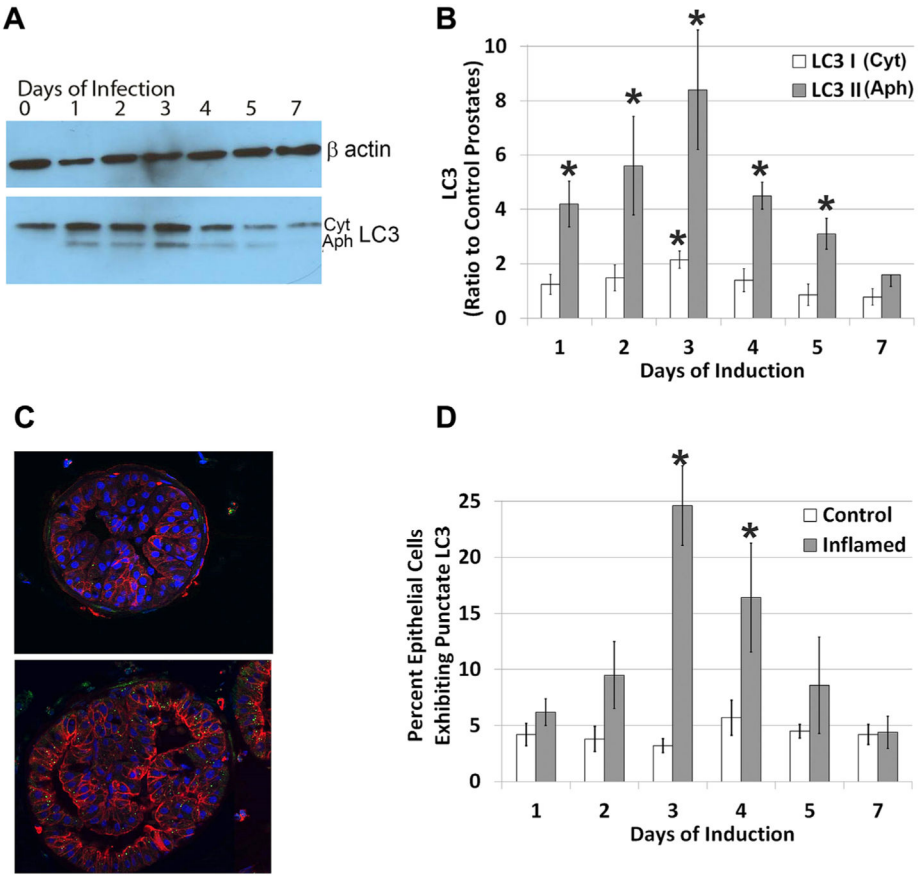

Fig. 5.

Inflammation autophagy marker expression in mouse dorsolateral prostates. **A**: Immunoblot example of induction of the autophagy marker LC3 at inflammation time points indicated; the higher running band (cyt) represents cytosolic LC3 while the lower running band (Aph) indicates LC3 associated in the autophagasome, and is indicative of autophagy induction. **B**: Quantified data of relative expression of all cytosolic and autophagasome-associated LC3; data were calculated as ratio of pixel intensity of the LC3 form, relative to β-actin, and expressed as ratio of expression to control prostates at the corresponding time of induction. Data are expressed as mean ±s.e.m. $^{*}P<0.05$ versus PBS-instilled (control) prostate; comparisons using analysis of variance (ANOVA), n =6. **C**: Immunofluorescence of LC3 (green) localization in 3 day instilled control (top) and inflamed (bottom) dorsolateral prostates demonstrating the characteristic punctate LC3 Localization with the autophagasome of autophagic epithelial cells, a further indicator of autophagic cells (PanCK, red). **D**: Quantified cell counting of epithelial cells positive for punctate LC3 Localization; data expressed are the percentage of epithelial cells expressing punctate LC3 in control and inflamed prostates at each time point of inflammation. All data are expressed as mean ±s.e.m. $^{*}P<0.05$ versus PBS-instilled prostate; comparisons using analysis of variance (ANOVA), n =6.

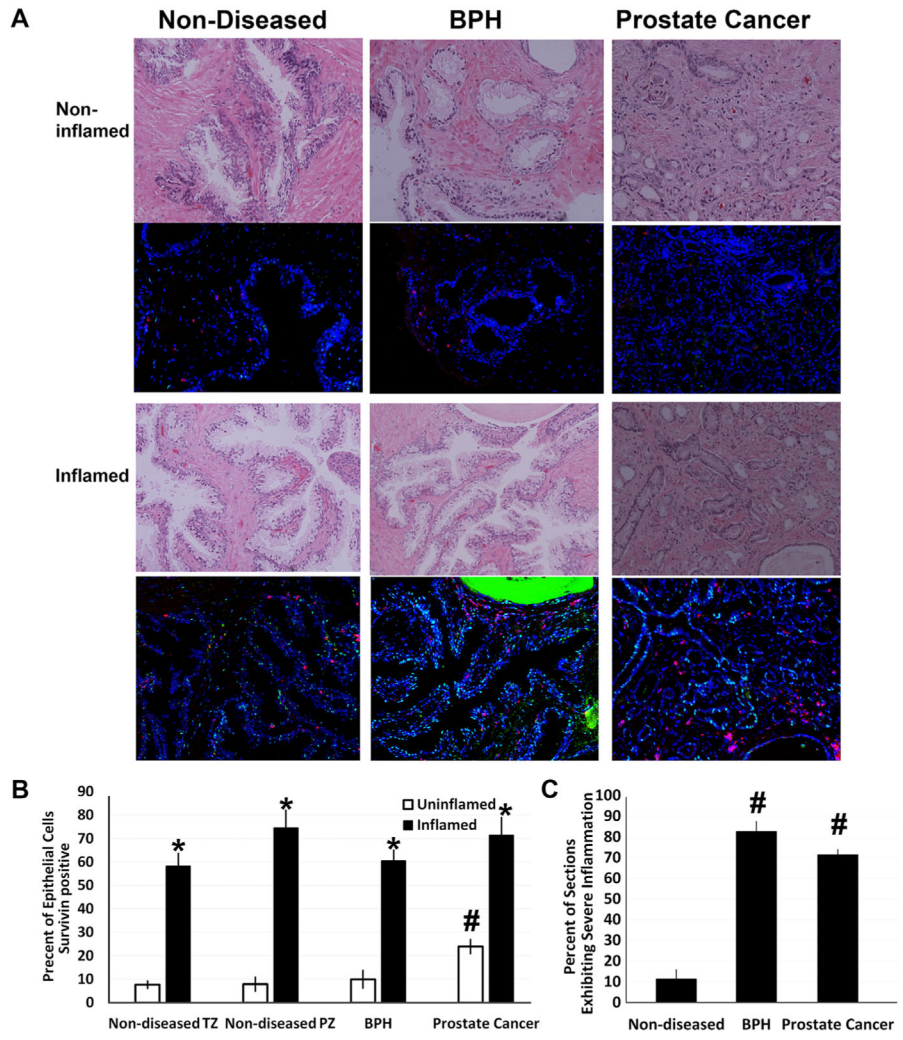

Fig. 6.

Human prostate specimens demonstrate intense survivin staining juxtaposed to regions of inflammation. **A**: Immunofluorescent images of non-inflamed or inflamed human prostates representing non-diseased controls (peripheral zone) taken from cystoprostatectomy cancer and BPH-free prostate specimens, BPH specimens (transition zone from TURP), or prostate cancer specimens, as indicated. Sections were stained for survivin (green) and CD45, a pan leukocyte marker (red) to identify regions of inflammation. Sections were deemed non-inflamed if they exhibited less than 10 Leukocytes per 20× field, and inflamed if they exhibited greater than 30 Leukocytes per field. **B**: Quantified cell counting of epithelial cells positive for survivin expression in human prostates; data expressed are the percentage of epithelial cells expressing survivin in non-inflamed and inflamed prostates at each time point of inflammation—three 20× fields per prostate section were averaged for each data point, and all data are expressed as mean ±s.e.m. $^{*}P$ <0.05 inflamed versus non-inflamed prostate; #P <0.05 disease condition versus non-diseased control. Analysis of variance (ANOVA), n =12 human prostates. **C**: percent of sections from each human prostate group (non-diseased, BPH, and cancer) that exhibited 30 Leukocytes per 20× section. Three 20× fields per

prostate section were averaged for each data point, and all data are expressed as mean ±s.e.m. $^{\#}P<0.05$, disease condition versus non-diseased control. Analysis of variance (ANOVA), n =12 human prostates.